Time domain localized-density-matrix method

Satoshi Yokojima, GuanHua Chen

Department of Chemistry, The University of Hong Kong, Pokfulam Road, Hong Kong, Hong Kong

Received 26 February 1998; accepted 11 June 1998

Abstract

A recently developed linear scaling localized-density-matrix method is modified, and the equation of motion for reduced single electron density matrix is solved for the absorption spectra of polyacetylene oligomers in the time-domain. The modified method requires much less computer memory which enables us to calculate linear optical response of larger oligomers containing up to 2000 carbon atoms. Different values of critical lengths are employed in the calculations, and their roles are clarified. © 1998 Elsevier Science B.V. All rights reserved.

Ab initio molecular orbital calculations are usually limited to small and medium size molecular systems. The obstacle lies in the rapid increasing of computational cost as the systems become larger and more complex. The computational time is proportional to a certain power of the system size, i.e., $t_{cpu} \propto N^x$, where t_{cpu} is the computational time, N is the number of electronic orbitals, and x is some number which is usually larger than 1. For instance, the computational time of ab initio Hartree–Fock molecular orbital calculation has an $O(N^3)$ scaling. This obstacle has been removed in principle. Several linear scaling methods have been developed to calculate electronic ground states [1–18]. Recently a localized-density-matrix method has been developed to calculate the excited state properties of very large electronic systems [19], and its computational time scales linearly with system size. It is based on the time-dependent Hartree–Fock (TDHF) approximation, and has been applied successfully to evaluate absorption spectra of polyacetylene oligomers containing up to 500 carbon atoms.

In Ref. [19] the equations of motion for density matrix in the localized-density-matrix method has been solved in the frequency domain. We refer it as the frequency domain localized-density-matrix method. Although the memory of calculation scales linearly with the size (N) of system, it is still quite large and is approximately proportional to $\alpha^3 N$, where α is a critical length [19]. The required memory is caused by a reduced Liouville matrix and becomes a major limiting factor for investigating larger systems. However, the Liouville matrix is not required if the equation of motion for the density matrix is solved in the time domain. This leads to a great reduction of memory requirement, and may enable us to solve the excited state properties of larger systems.

In the present Letter we modify the frequency domain localized-density-matrix method and follow the propagation of the reduced single-electron density matrix in the time domain. The modified method is referred to as the time domain localized-density-matrix method, and is applied to calculate the optical

absorption spectra of polyacetylene oligomers containing up to 2000 carbon atoms.

When an external electromagnetic field $\mathscr{E}(t)$ is applied to a polyacetylene oligomer, its π electrons response to the field, and optical signals may be observed. The π electrons in the polyacetylene are well described by the PPP Hamiltonian [20–22],

$$H = H_{SSH} + H_C + H_{ext}. \tag{1}$$

H_{SSH} is the Su–Schrieffer–Heeger (SSH) Hamiltonian, which consists of the Hückel Hamiltonian plus electron-phonon coupling. H_C represents the Coulomb interaction among the π electrons. H_{ext} is the interaction between the π electrons and an external electric field $\mathscr{E}(t)$. We employ the same parameters as in Ref. [19], except that $\bar{x} = 1.59$ Å. The geometry is fixed in the calculation. Here N π-orbitals of N carbon atoms are employed as the basis set, and m and n represent π-orbitals at the sites m and n, respectively. With the TDHF approximation [23], a closed nonlinear self-consistent equation of motion are yielded for the reduced single-electron density matrix $\rho(t)$,

$$i\hbar \dot{\rho}(t) = [h(t) + f(t), \rho(t)]. \tag{2}$$

Here $h(t)$ is the Fock matrix, and $f(t)$ describes the interaction between an electron and the external field $\mathscr{E}(t)$ [20].

We partition the density matrix $\rho(t)$ into two parts:

$$\rho(t) = \rho^{(0)} + \delta\rho(t), \tag{3}$$

where $\rho^{(0)}$ is the reduced density matrix representing the Hartree–Fock ground state in the absence of external fields, and $\delta\rho(t)$ is the difference between $\rho(t)$ and $\rho^{(0)}$, i.e., the induced density matrix by the external field $\mathscr{E}(t)$. Similarly, the Fock operator $h(t)$ is decomposed in the form,

$$h(t) = h^{(0)} + \delta h(t), \tag{4}$$

where $h^{(0)}$ is the Fock matrix when $\mathscr{E}(t) = 0$:

$$h^{(0)}_{nm} = t_{nm} + \delta_{n,m} \sum_l v_{nl} \rho^{(0)}_{ll} - v_{nm} \rho^{(0)}_{nm}, \tag{5}$$

where t_{nm} is the hopping matrix element between m and n, and v_{nm} is the Coulomb repulsion between two electrons at m and n, respectively.

We concentrate on investigating the linear response to $\mathscr{E}(t)$. For first-order induced density ma-

trix $\delta\rho^{(1)}$ in $\mathscr{E}(t)$, its dynamics may be described by the following equation,

$$
\begin{aligned}
i\hbar \, \delta\dot{\rho}^{(1)}_{i,j} =\ & \sum_k \left(h^{(0)}_{i,k} \delta\rho^{(1)}_{k,j} - \delta\rho^{(1)}_{i,k} h^{(0)}_{k,j} \right) \\
& + 2 \sum_k \left(v_{i,k} - v_{j,k} \right) \rho^{(0)}_{i,j} \delta\rho^{(1)}_{kk} \\
& - \sum_k \left(v_{i,k} \rho^{(0)}_{j,k} \delta\rho^{(1)}_{i,k} - v_{j,k} \rho^{(0)}_{i,k} \delta\rho^{(1)}_{k,j} \right) \\
& + e(z(i) - z(j)) \mathscr{E}(t) \rho^{(0)}_{i,j}.
\end{aligned} \tag{6}
$$

Eq. (6) is integrated in the time domain. Most matrix elements of $h^{(0)}$, $\rho^{(0)}$ and $\delta\rho^{(1)}$ are virtually zero when N is large enough. Just as in Ref. [19], we employ the following approximations by introducing three critical lengths α_0, α_1 and α_c:

(1) $h^{(0)}_{i,j} = 0$, $\rho^{(0)}_{i,j} = 0$ if $|i - j| > \alpha_0$;

(2) $\delta\rho^{(1)}_{i,j} = 0$ if $|i - j| > \alpha_1$;

and for the second term on the right hand side (RHS) of Eq. (6),

(3) $v_{i,j} = 0$ if $|i - j| > \alpha_c$.

The approximation (3) makes use of the cancellations among the second term of the RHS of Eq. (6). The cancellations ensure that $\delta\dot{\rho}^{(1)}_{i,j}(t) \approx 0$ for $|i - j| > \alpha_1$ ($\alpha_1 \geq \alpha_c$). Thus

$$
\begin{aligned}
i\hbar \, \delta\dot{\rho}^{(1)}_{i,j} =\ & \sum_k^{|i-k| \leq \alpha_0, |k-j| \leq \alpha_1} h^{(0)}_{i,k} \delta\rho^{(1)}_{k,j} \\
& - \sum_k^{|i-k| \leq \alpha_1, |k-j| \leq \alpha_0} \delta\rho^{(1)}_{i,k} h^{(0)}_{k,j} \\
& + 2 \sum_k^{k_0 \leq k \leq k_1} \left(v_{i,k} - v_{j,k} \right) \rho^{(0)}_{i,j} \delta\rho^{(1)}_{kk} \\
& - \sum_k^{|i-k| \leq \alpha_1, |k-j| \leq \alpha_0} v_{i,k} \rho^{(0)}_{j,k} \delta\rho^{(1)}_{i,k} \\
& + \sum_k^{|i-k| \leq \alpha_0, |k-j| \leq \alpha_1} v_{j,k} \rho^{(0)}_{i,k} \delta\rho^{(1)}_{k,j} + e(z(i) \\
& - z(j)) \mathscr{E}(t) \rho^{(0)}_{i,j},
\end{aligned} \tag{7}
$$

where k_0 and k_1 depend on i and j, and are determined as: $k_0 = \max(1, \min(i - \alpha_c, j - \alpha_c))$ and $k_1 = \min(\max(i + \alpha_c, j + \alpha_c), N)$.
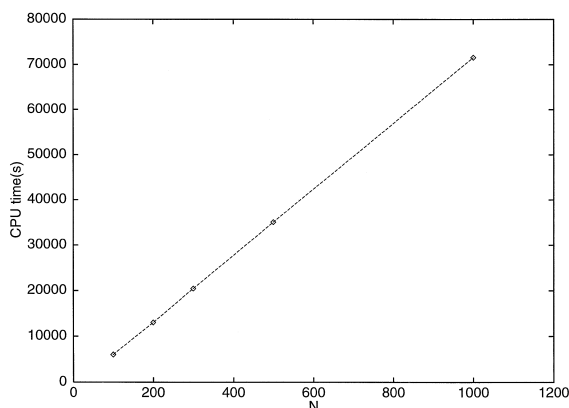
Fig. 1. CPU time on an SGI Indigo2 R10000 workstation for 100, 200, 300, 500 and 1000. Each calculation is performed during the time interval between -0.5 fs and 70 fs with the time step 0.01 fs. The phenomenological dephasing constant $\Gamma = 0.1$ eV. $\alpha_0 = \alpha_1 = \alpha_c = 24$.

The fourth-order Runge-Kutta method [24] is used to integrate Eq. (7). The external field employed is

$$\mathscr{E}(t) = \frac{1}{\sqrt{\pi}\,\bar{t}}\, e^{-(t/\bar{t})^2}, \tag{8}$$

where $\bar{t} = 0.1$ fs. The phenomenological dephasing constant is set to 0.1 eV.

To verify that the computational time scales linearly with the system size N, we propagate Eq. (7) between a time interval $[-0.5$ fs, 70 fs$]$ with a time step 0.01 fs for $N = 100$, 200, 300, 500 and 1000, and record the total CPU time for each N. The computational time spent in obtaining the Hartree–Fock ground state is subtracted from the total CPU time. The resulting computational time versus N is plotted in Fig. 1. Clearly, the CPU time is proportional to the system size N. The resulting $\delta\rho^{(1)}(t)$ may be used to obtain the absorption spectrum for each N by Fourier transform.

The values of α_0, α_1 and α_c are important for accurate determination of absorption spectrum and computational time. It has been observed in [19] that $\alpha_0 = \alpha_1 = \alpha_c = 20$ leads to satisfactory absorption spectrum between 1.5 and 3.6 eV for $N = 40$. Fig. 2a and 2b show the absorption spectrum for $N = 80$ with different α_0, α_1 and α_c. The same spectrum is plotted against different energy ranges in the two figures. The scale for the absorption intensity in Fig. 2a is 33 times of that in Fig. 2b. The solid line is for (a) $\alpha_0 = \alpha_1 = \alpha_c = 20$, the dashed line for (b) $\alpha_0 = \alpha_c = 20$ and $\alpha_1 = 30$, and the dotted line for (c) $\alpha_0 = \alpha_1 = \alpha_c = 40$. The results of the full TDHF calculation for $N = 80$ are given by diamonds. For $\omega = 1.8$ to 3.4 eV, the spectra for three sets of α_0 α_1 α_c critical lengths give almost exact result. It means that it is sufficient to use the critical lengths $\alpha_0 = \alpha_1 = \alpha_c = 20$ to calculate the absorption spectrum in
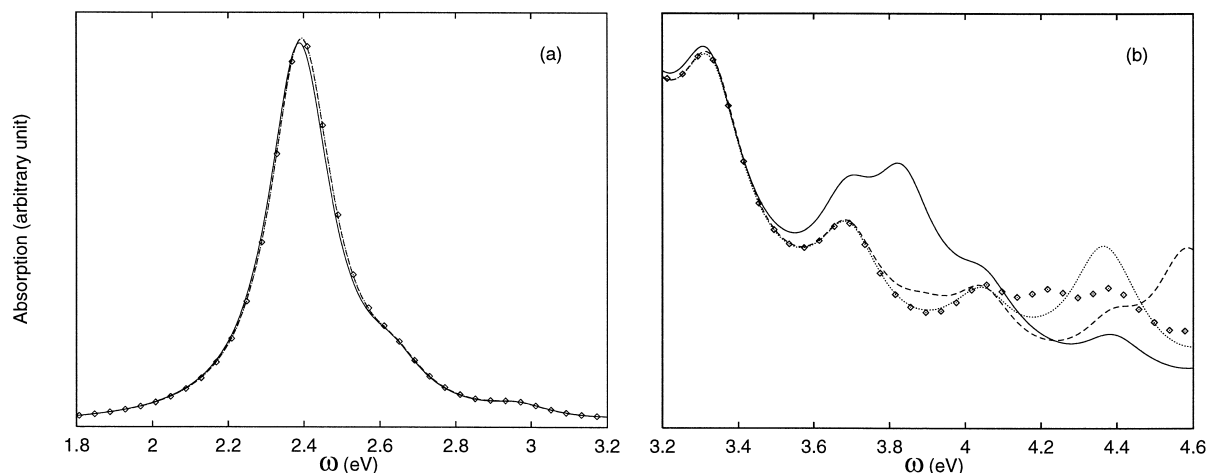

Fig. 2. Absorption spectra for $N = 80$. The solid line: $\alpha_0 = \alpha_1 = \alpha_c = 20$. The dashed line: $\alpha_0 = \alpha_c = 20$, and $\alpha_1 = 30$. The dotted line: $\alpha_0 = \alpha_1 = \alpha_c = 40$. The results of the full TDHF calculation for $N = 80$ are given by diamonds. The phenomenological dephasing constant $\Gamma = 0.1$ eV. The vertical scale of (a) is 33 times of the scale of (b).

this energy range. Starting from 3.4 eV the result of calculation (a) deviates from the exact values. Whereas the calculation (b) reproduces accurately exact result up to 3.8 eV, and calculation (c) yields accurate result up to 4.1 eV. Larger values of critical lengths α_0, α_1 and α_c lead to better spectrum in higher energy range. We calculate the absorption spectrum for $N = 80$ by employing $\alpha_0 = \alpha_1 = \alpha_c = 30$, and the resulted spectrum is almost the same as that of (b). Thus, we conclude that the calculated properties of higher excited states are more sensitive to α_1. This is consistent with the fact that the higher excited states have larger critical lengths than the lower excited states. To determine optical spectrum of higher energy range, larger value of α_1 is required.

In Fig. 3, we plot the absorption spectra for $N = 100$, 200, 500 and 2000. For comparison, all data are multiplied a factor $2000/N$. As N increases, the absorption peak red shifts toward the bulk value and the absorption spectrum become smoother. In the inset the amplitude of absorption peak is plotted versus N. It is observed that the amplitude scales linearly with N to the zero order in $1/N$. This is consistent with the work of Mukamel and coworkers [25].
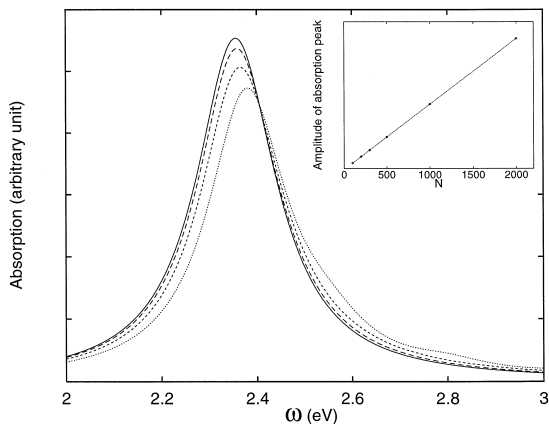
Eq. (7) has been solved in the frequency domain,

see Ref. [19]. In the frequency domain, the matrix involved is a sparse matrix, and moreover, is band diagonal. Therefore, a Gaussian elimination procedure with backsubstitution was used, and the linear scaling of the computational time was achieved. However, for two or three dimensional systems, the sparse matrix is no longer band diagonal. Different linear scaling procedures are required. For instance, iterative conjugated gradient method may be used [24].

To summarize, the equation of motion for the truncated reduced single electron density matrix have been solved in the time domain, and the calculation time scales linearly with the system size. Compared with the frequency domain localized-density-matrix method in Ref. [19], the current method requires much less computer memory, and thus, the excited state properties of larger systems may be calculated.

Acknowledgements

References

[1] W. Yang, Phys. Rev. Lett. 66 (1991) 1438.
[2] W. Yang, T.-S. Lee, J. Chem. Phys. 103 (1995) 5674.
[3] P. Cortona, Phys. Rev. B 44 (1991) 8454.
[4] G. Galli, M. Parrinello, Phys. Rev. Lett. 69 (1992) 3547.
[5] S. Baroni, P. Giannozzi, Europhys. Lett. 17 (1992) 547.
[6] X.-P. Li, R.W. Nunes, D. Vanderbilt, Phys. Rev. B 47 (1993) 10891.
[7] F. Mauri, G. Galli, R. Car, Phys. Rev. B 47 (1993) 9973.
[8] P. Ordejón, D.A. Drabold, M.P. Grumbach, R.M. Martin, Phys. Rev. B 48 (1993) 14646.
[9] W. Kohn, Chem. Phys. Lett. 208 (1993) 167.
[10] D.A. Drabold, O.F. Sankey, Phys. Rev. Lett. 70 (1993) 3631.
[11] A. Gibson, R. Haydock, J.P. LaFemina, Phys. Rev. B 47 (1993) 9229.
[12] M. Aoki, Phys. Rev. Lett. 71 (1993) 3842.
[13] E.B. Stechel, A.P. Williams, P.J. Feibelman, Phys. Rev. B 49 (1994) 10088.
[14] S. Goedecker, L. Colombo, Phys. Rev. Lett. 73 (1994) 122.
[15] J.P. Stewart, Int. J. Quant. Chem. 58 (1995) 133.
[16] M.C. Strain, G.E. Scuseria, M.J. Frisch, Science 271 (1996) 51.
[17] S.L. Dixon, K.M. Merz Jr., J. Chem. Phys. 104 (1996) 6643.

Fig. 3. Absorption spectra for $N = 100$, 200, 500 and 2000. $\alpha_0 = \alpha_1 = \alpha_c = 24$. The phenomenological dephasing constant $\Gamma = 0.1$ eV. For comparison, all data are multiplied by $2000/N$. The solid, long dashed, short dashed and dotted lines are for $N = 100$, 200, 500 and 2000, respectively. The inset shows the linear scaling of the amplitude of first absorption peak.

[18] E. Schwegler, M. Challacombe, M. Head-Gordon, J. Chem. Phys. 106 (1997) 9708.

[19] S. Yokojima, G.H. Chen, Phys. Rev. Lett., submitted.

[20] A. Takahashi, S. Mukamel, J. Chem. Phys. 100 (1994) 2366.

[21] H. Fukutome, J. Mol. Struct. (Theochem) 188 (1989) 337.

[22] Z.G. Soos, S. Ramesesha, D.S. Galvao, S. Etemad, Phys. Rev. B 47 (1993) 1742.

[23] P. Ring, P. Schuck, The Nuclear Many-Body Problem (Springer, New York, 1980).

[24] W.H. Press, B.P. Flannery, S.A. Teukolsky, W.T. Vetterling, Numerical Recipes in C (Cambridge University Press, New York, 1988).

[25] S. Tretiak, V. Chernyak, S. Mukamel, Phys. Rev. Lett. 77 (1996) 4656.